electronic reprint

STRUCTURAL CHEMISTRY

ISSN: 2053-2296
journals.iucr.org/c

Synthesis, structural characterization and computational studies of *catena*-poly[chlorido[μ_3-(pyridin-1-ium-3-yl)phosphonato-$\kappa^3 O:O':O''$]zinc(II)]

Magdalena Wilk-Kozubek, Katarzyna N. Jarzembska, Jan Janczak and Veneta Videnova-Adrabinska

Acta Cryst. (2017). C**73**, 363–368

IUCr Journals
CRYSTALLOGRAPHY JOURNALS ONLINE

Copyright © International Union of Crystallography

Author(s) of this paper may load this reprint on their own web site or institutional repository provided that this cover page is retained. Republication of this article or its storage in electronic databases other than as specified above is not permitted without prior permission in writing from the IUCr.

For further information see http://journals.iucr.org/services/authorrights.html

Acta Cryst C STRUCTURAL CHEMISTRY

ISSN 2053-2296

Synthesis, structural characterization and computational studies of *catena*-poly[chlorido-[μ_3-(pyridin-1-ium-3-yl)phosphonato-κ^3O:O':O'']-zinc(II)]

Magdalena Wilk-Kozubek,[a,b]* Katarzyna N. Jarzembska,[c] Jan Janczak[d] and Veneta Videnova-Adrabinska[a]*

[a]Department of Chemistry, Wrocław University of Science and Technology, 27 Wybrzeże Wyspiańskiego Street, 50-370 Wrocław, Poland, [b]Department of Nanotechnology, Wrocław Research Centre EIT+, 147 Stabłowicka Street, 54-066 Wrocław, Poland, [c]Department of Chemistry, University of Warsaw, 101 Żwirki i Wigury Street, 02-089 Warsaw, Poland, and [d]Institute of Low Temperature and Structure Research, Polish Academy of Sciences, PO Box 1410, 2 Okólna Street, 50-950 Wrocław, Poland. *Correspondence e-mail: magdalena.wilk@eitplus.pl, veneta.videnova-adrabinska@pwr.edu.pl

Received 24 January 2017
Accepted 21 March 2017

Edited by N. Lugan, Laboratoire de Chimie de Coordination du CNRS, Toulouse, France

Keywords: phosphonic acid; one-dimensional coordination polymer; single-crystal X-ray diffraction; periodic DFT calculations; vibrational spectroscopy; zinc(II) complex; computational chemistry.

CCDC reference: 1524251

Supporting information: this article has supporting information at journals.iucr.org/c

Coordination polymers are constructed from two basic components, namely metal ions, or metal-ion clusters, and bridging organic ligands. Their structures may also contain other auxiliary components, such as blocking ligands, counter-ions and nonbonding guest or template molecules. The choice or design of a suitable linker is essential. The new title zinc(II) coordination polymer, $[Zn(C_5H_5NO_3P)Cl]_n$, has been hydrothermally synthesized and structurally characterized by single-crystal X-ray diffraction and vibrational spectroscopy (FT–IR and FT–Raman). Additionally, computational methods have been applied to derive quantitative information about interactions present in the solid state. The compound crystallizes in the monoclinic space group $C2/c$. The four-coordinated Zn^{II} cation is in a distorted tetrahedral environment, formed by three phosphonate O atoms from three different (pyridin-1-ium-3-yl)phosphonate ligands and one chloride anion. The Zn^{II} ions are extended by phosphonate ligands to generate a ladder chain along the [001] direction. Adjacent ladders are held together *via* N—H···O hydrogen bonds and offset face-to-face π–π stacking interactions, forming a three-dimensional supramolecular network with channels. As calculated, the interaction energy between the neighbouring ladders is -115.2 kJ mol^{-1}. In turn, the cohesive energy evaluated per asymmetric unit-equivalent fragment of a polymeric chain in the crystal structure is -205.4 kJ mol^{-1}. This latter value reflects the numerous hydrogen bonds stabilizing the three-dimensional packing of the coordination chains.

1. Introduction

Over the past two decades, coordination polymers have emerged as a new class of functional materials. They have attracted considerable attention due to their interesting structures (O'Keeffe & Yaghi, 2012), as well as their potential applications in many strategic fields, such as gas storage (Suh *et al.*, 2012), gas purification and separation (Li *et al.*, 2012), heterogeneous catalysis (Lee *et al.*, 2009), targeted drug delivery (Horcajada *et al.*, 2012), sensing (Kreno *et al.*, 2012) and magnetism (Kurmoo, 2009). Coordination polymers are constructed from two basic components, namely metal ions, or metal-ion clusters, and bridging organic ligands. However, their structures may also contain other auxiliary components, such as blocking ligands, counter-ions and nonbonding guest or template molecules (Kitagawa *et al.*, 2004).

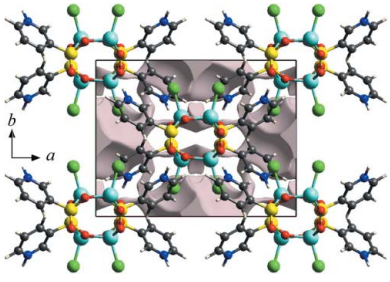

© 2017 International Union of Crystallography

electronic reprint

For the successful preparation of coordination polymers, the choice or design of a proper linker is essential. In this work, we have investigated the use of rigid pyridin-3-yl-phosphonic acid (H_2L) (Zoń *et al.*, 2011) as the organic ligand. H_2L exhibits a strong binding ability, since the phosphonic acid group itself is capable of linking up to nine metal ions and the pyridyl N atom provides an additional binding site. Furthermore, the use of the rigid ligand favours the formation of crystalline coordination polymers (Białek *et al.*, 2013). So far, H_2L has been employed to form the following coordination polymers: $[ZnBr(HL)]_n$ and $[Sn(L)]_n$ (one-dimensional ladder structures; Ayyappan *et al.*, 2001; Perry *et al.*, 2010), $[Cu(L)]_n$ (a two-dimensional layer structure; Zhou *et al.*, 2010), $[Co(L)]_n$ (a three-dimensional pillared-layer structure; Wasson & LaDuca, 2007) and $\{[Cd(HL)_2]\cdot DMSO\}_n$ (a three-dimensional open-framework structure; DMSO is dimethyl sulfoxide; Ayyappan *et al.*, 2001).

This paper presents the results of the synthesis, structural characterization and computational analysis of a new zinc(II) coordination polymer, namely *catena*-poly[chlorido[μ_3-(pyridin-1-ium-3-yl)phosphonato-κ^3O:O':O'']zinc(II)], (1), which enriches our knowledge about the family of one-dimensional coordination polymers based on the H_2L acid.

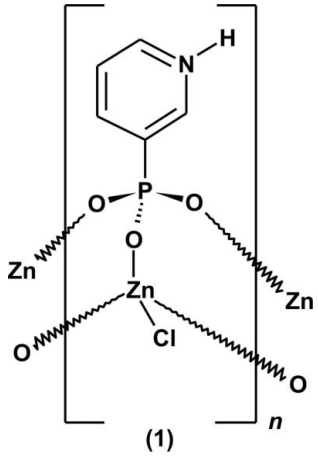

(1)

2. Experimental

All chemicals were of AR grade and were used without further purification. The ^{1}H NMR spectrum was acquired at room temperature on a Bruker Avance DRX-300 spectrometer at 300.13 MHz with tetramethylsilane as the standard. The $^{31}P\{^1H\}$ NMR spectrum was recorded on the same instrument at 121.50 MHz. Standard CHN elemental analysis was carried out on an Elementar vario EL III elemental analyzer.

2.1. Synthesis and crystallization

2.1.1. Preparation of pyridin-3-ylphosphonic acid (H_2L). Diethyl pyridin-3-ylphosphonate was prepared according to the procedure of Zoń *et al.* (2011) from 3-bromopyridine (0.616 ml, 6.33 mmol), diethyl phosphite (0.989 ml, 7.60 mmol), triethylamine (1.059 ml, 7.60 mmol), toluene (10 ml) and tetrakis(triphenylphosphine)palladium(0) (0.292 g, 0.253 mmol). The phosphonate ester was then treated with concentrated hydrochloric acid (7 ml) and refluxed for 24 h. After hydrolysis, the reaction mixture was extracted with methylene chloride (2 × 5 ml). The aqueous layer was concentrated under reduced pressure. Distilled water (5 ml) was then added and the resulting mixture was evaporated to dryness. The residue was treated with methanol (15 ml) and concentrated hydrochloric acid (0.528 ml) and heated under reflux on a water bath to achieve complete dissolution. After cooling, the product was precipitated by adding excess (±)-propylene oxide. A white precipitate of pyridin-3-ylphosphonic acid was collected by suction, washed with methanol (3 × 2 ml), dried under reduced pressure and recrystallized from a water–methanol mixture (1:1 *v*/*v*, 6 ml) (yield 0.679 g, 67%). ^{1}H NMR (300.13 MHz, D_2O): δ 8.77–8.59 (*m*, 3H, aromatic H), 7.98–7.93 (*m*, 1H, aromatic H). $^{31}P\{^1H\}$ NMR (121.50 MHz, D_2O): δ 4.05 (*s*).

Table 1
Experimental details.

Crystal data	
Chemical formula	$[Zn(C_5H_5NO_3P)Cl]$
M_r	258.89
Crystal system, space group	Monoclinic, *C*2/*c*
Temperature (K)	295
a, *b*, *c* (Å)	15.260 (3), 11.750 (2), 10.334 (2)
β (°)	99.04 (3)
V (Å^3)	1830.0 (7)
Z	8
Radiation type	Mo *K*α
μ (mm^{-1})	3.12
Crystal size (mm)	0.22 × 0.15 × 0.12
Data collection	
Diffractometer	Kuma KM-4-CCD
Absorption correction	Multi-scan (*CrysAlis PRO*; Rigaku Oxford Diffraction, 2015)
T_{min}, T_{max}	0.832, 1.000
No. of measured, independent and observed [$I > 2\sigma(I)$] reflections	11615, 2323, 1633
R_{int}	0.048
$(\sin \theta/\lambda)_{max}$ (Å^{-1})	0.689
Refinement	
$R[F^2 > 2\sigma(F^2)]$, $wR(F^2)$, *S*	0.035, 0.071, 1.00
No. of reflections	2323
No. of parameters	112
H-atom treatment	H atoms treated by a mixture of independent and constrained refinement
$\Delta\rho_{max}$, $\Delta\rho_{min}$ (e Å^{-3})	0.87, −0.45

Computer programs: *CrysAlis CCD* (Rigaku Oxford Diffraction, 2015), *CrysAlis RED* (Rigaku Oxford Diffraction, 2015), *SHELXT* (Sheldrick, 2015*a*), *SHELXL2014* (Sheldrick, 2015*b*) and *DIAMOND* (Brandenburg & Putz, 2006).

2.1.2. Preparation of $[ZnCl(HL)]_n$, (1). A solution of pyridin-3-ylphosphonic acid (30.0 mg, 0.188 mmol) in distilled water (1 ml) was mixed with zinc(II) chloride (25.6 mg, 0.188 mmol), also dissolved in distilled water (1 ml). The resulting solution was placed in a 45 ml Parr reactor and heated at 413 K for 24 h. The mixture was then cooled to room temperature and colourless parallelepiped-shaped crystals of (1) were obtained. These crystals were collected by gravity filtration, washed with distilled water (3 × 0.5 ml) and dried in air (yield 1.0 mg, 2% based on Zn). Analysis found (calculated) for $C_5H_5ClNO_3PZn$ (%): C 22.75 (23.19), H 1.94 (1.95), N 5.36 (5.41).

electronic reprint

2.2. Vibrational spectroscopy

The FT–IR spectrum of compound (1) was recorded on a Bruker Vertex 70v FT–IR spectrometer in the range 4000–370 cm^{-1}, with a resolution of 2 cm^{-1}, using the KBr pellet technique. The FT–Raman spectrum of (1) was collected on a Bruker MultiRAM FT–Raman spectrometer in the range 3600–50 cm^{-1}, with a resolution of 2 cm^{-1}, using the Nd:YAG laser line at 1064 nm. Instrument control and spectra analysis were performed using the Bruker *OPUS* software.

2.3. Refinement

Crystal data, data collection and structure refinement details are summarized in Table 1. The positions of the H atoms attached to C atoms were constrained to C—H = 0.93 Å and $U_{iso}(H) = 1.2U_{eq}(C)$. The H atom bonded to the N atom was refined with $U_{iso}(H) = 1.2U_{eq}(N)$.

2.4. Computational details

All energy computations were performed using the *CRYSTAL09* program package (Dovesi *et al.*, 2009) at the DFT(B3LYP) level of theory (Becke, 1988; Dunning, 1989; Lee *et al.*, 1988) with the 6-31G** molecular all-electron basis set (Krishnan *et al.*, 1980). Starting input files were prepared using the *CLUSTERGEN* program (Kamiński *et al.*, 2013). The crystal structure of (1) was optimized prior to the computational analysis, so as to obtain reliable H-atom positions (Jarzembska *et al.*, 2012). During the optimization procedure, only the atomic positions were varied, while the unit-cell parameters were kept fixed at the experimental values.

The cohesive-like energy computation was carried out according to a slight modification of a standard procedure described in the literature (Civalleri *et al.*, 2008; Jarzembska *et al.*, 2012). Both Grimme dispersion correction (Civalleri *et al.*, 2008; Grimme, 2011) and correction for basis set superposition error (BSSE) (Boys & Bernardi, 1970) were applied. Instead of a molecule, a polymeric substructure was chosen (a polymeric chain along the [001] direction). The closest polymeric fragments to the central species were considered as ghost atoms, and were used for the BSSE estimation. The evaluation of Coulomb and exchange series was controlled by five thresholds, set arbitrarily to the values of 10^{-7}, 10^{-7}, 10^{-7}, 10^{-7} and 10^{-25}. The shrinking factor was equal to 8. The cohesive energy (E_{coh}) was calculated as described below:

$$E_{coh} = \frac{1}{Z} E_{bulk} - E_{pol},$$

where E_{bulk} is the total energy of a system (calculated per unit cell) and E_{pol} is the energy of a polymer extracted from the bulk. Z stands for the number of polymeric fragments in the unit cell. The final energy was scaled to the asymmetric unit (ASU)-equivalent fragment of the polymeric chain.

When exploring the polymeric substructure interactions, the POLYMER option available in the *CRYSTAL09* package was used, which enabled application of the periodic boundary. For that purpose, the crystal structure fractional coordinates of a unit molecular fragment were transformed to a $p1$ rod group of symmetry with the lattice vector of 10.334 Å set along the x direction, so as to match the *CRYSTAL09* program requirement (in the input file, the coordinates along the lattice vector are fractional, whereas the transformed coordinates along the y and z directions are given in Å units). A similar procedure to that mentioned above was used by Durka *et al.* (2012). A supermolecular approach was employed to derive the interaction energy values. In all cases, the BSSE correction did not exceed 10% of the final energy value.

3. Results and discussion

Compound (1) was obtained by hydrothermal reaction between zinc(II) chloride and pyridin-3-ylphosphonic acid at 413 K and its formation was confirmed by two complementary spectroscopic techniques, *viz.* FT–IR and FT–Raman spectroscopy. The IR and Raman spectra of (1) are presented in Fig. S1 of the *Supporting information*. No bands are observed in the IR spectrum in the regions 2700–2560 and 2300–2100 cm^{-1}, indicating that there are no phosphonic acid O—H stretching vibrations (Socrates, 2001) in (1). Thus, the two strongest bands near 1105 and 1025 cm^{-1} can be attributed to the asymmetric and symmetric stretching vibrations of the phosphonate group (Zhou *et al.*, 2010). In turn, the bands in the range 640–370 cm^{-1} can be ascribed to the PO_3 deformation vibrations. The band above 3425 cm^{-1}, similar to that found for H_2L, can be assigned to the N—H stretching vibration of the pyridinium group involved in a hydrogen-bonding interaction (Zoń *et al.*, 2011). The corresponding N—H deformation vibration appears as a very intense band around 1170 cm^{-1}. Additionally, some bands are characteristic for the stretching and deformation vibrations of the pyridin-

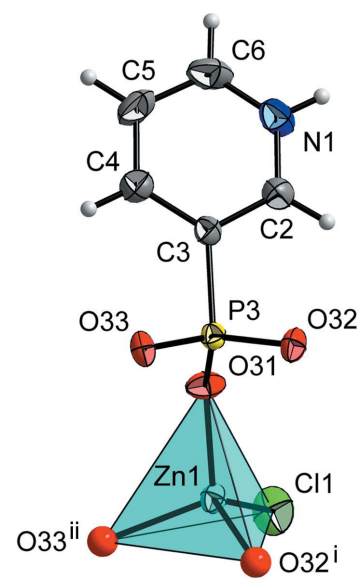

Figure 1
The asymmetric unit and the coordination polyhedron of the Zn^{II} ion in the crystal structure of (1), together with the atom-labelling scheme. The displacement ellipsoids are drawn at the 50% probability level. [Symmetry codes: (i) $-x + 1, y, -z + \frac{1}{2}$; (ii) $-x + 1, -y + 1, -z$.]

electronic reprint

Table 2
Selected geometric parameters (Å, °).

Zn1—O31	1.9390 (19)	P3—O32	1.5195 (19)
Zn1—O32^{i}	1.9406 (19)	P3—O33	1.527 (2)
Zn1—O33^{ii}	1.9817 (19)	P3—C3	1.825 (3)
Zn1—Cl1	2.2249 (10)	N1—C6	1.315 (4)
P3—O31	1.508 (2)	N1—C2	1.348 (4)
O31—Zn1—O32^{i}	110.24 (8)	O33^{ii}—Zn1—Cl1	103.54 (6)
O31—Zn1—O33^{ii}	108.85 (9)	O31—P3—O32	115.04 (12)
O32^{i}—Zn1—O33^{ii}	104.83 (8)	O31—P3—O33	113.29 (12)
O31—Zn1—Cl1	110.66 (7)	O32—P3—O33	109.91 (12)
O32^{i}—Zn1—Cl1	118.03 (7)	C6—N1—C2	122.4 (3)

Symmetry codes: (i) $-x+1, y, -z+\frac{1}{2}$; (ii) $-x+1, -y+1, -z$.

ium aromatic ring. Three bands in the region 3125–3050 cm^{-1} are attributed to the aromatic C—H stretching vibrations. The bands of medium-to-strong intensity in the ranges 1620–1535 and 1485–1380 cm^{-1} are associated with the ring C═C and C═N stretching vibrations, respectively. Several bands of variable intensity in the regions 1220–1000 and 820–715 cm^{-1} are due to the in-plane and out-of-plane C—H deformation vibrations, respectively. Finally, two bands in the range 715–640 cm^{-1} arise from the in-plane and out-of-plane ring deformation vibrations. The positions and intensities of all observed vibrational modes together with their tentative assignments are given in Table S1 (see *Supporting information*).

The solid-state structure of (1) was established by single-crystal X-ray diffraction analysis. It revealed that the compound crystallizes in the monoclinic *C*2/*c* space group. The asymmetric unit of (1) contains one Zn^{II} cation, one (pyridin-1-ium-3-yl)phosphonate monoanionic ligand and one chloride ligand. The Zn^{II} ion is four-coordinated with a distorted tetrahedral geometry. The coordination environment of the Zn^{II} ion consists of three phosphonate O atoms from three (pyridin-1-ium-3-yl)phosphonate ligands and one chloride ligand (Fig. 1). The Zn1—O bond lengths vary from 1.9390 (19) to 1.9817 (19) Å, while the Zn1—Cl1 bond length is 2.2249 (10) Å (Table 2). The bond angles around the Zn^{II} ion range from 103.54 (6) to 118.03 (7)°. The bond lengths and angles within the $[ZnO_3Cl]$ tetrahedron are in agreement with those reported for other chloride-containing zinc(II) phosphonates (Fry *et al.*, 2008; Liu *et al.*, 2008; Samanamu *et al.*, 2008).

The (pyridin-1-ium-3-yl)phosphonate monoanion acts as a tridentate ligand. Each phosphonate group bridges three neighbouring Zn^{II} cations in a η^3-μ_3 fashion, leading to the formation of a ladder structure along the [001] direction (Fig. 2). The polymeric chain is composed of repeating *R*2,4(8) coordination motifs [for the definition of the notation for coordination motifs, see Matczak-Jon & Videnova-Adrabińska (2005)]. The Zn1···Zn1 distances between the rotation- and inversion-related ions are 4.0999 (13) and 4.2375 (8) Å, respectively. The ladder structure is additionally supported by weak C2—H2···Cl1^{i} hydrogen bonds (see Table 3 for hydrogen-bond details and symmetry code). According to the notation of Cheetham *et al.* (2006), the presented structure can be described as I^1O^0 with respect to

Table 3
Hydrogen-bond geometry (Å, °).

D—H···*A*	*D*—H	H···*A*	*D*···*A*	*D*—H···*A*
C2—H2···Cl1^{i}	0.93	2.85	3.756 (3)	164
N1—H1N···O33^{iii}	0.91 (4)	1.85 (4)	2.756 (4)	175 (3)
C6—H6···O31^{iv}	0.93	2.57	3.134 (4)	120

Symmetry codes: (i) $-x+1, y, -z+\frac{1}{2}$; (iii) $-x+\frac{3}{2}, y-\frac{1}{2}, -z+\frac{1}{2}$; (iv) $-x+\frac{3}{2}, -y+\frac{1}{2}, -z$.

the inorganic and organic connectivity. There are two reasons explaining why compound (1) exhibits a low-dimensional coordination structure. The first is that the fourth coordination position around the Zn^{II} ion is occupied by the terminal chloride ligand and, as a consequence, this position is not available for the bridging phosphonate ligand. The second reason is that the N atom of the pyridyl group is protonated and, as a result, is unable to bind the Zn^{II} ion. However, the presence of hydrogen-bond donors and acceptors and aromatic moieties gives the possibility of organizing the coordination chains into a higher-dimensional supramolecular architecture by hydrogen-bonding and π–π stacking interactions.

Hence, adjacent ladders are interconnected by relatively strong N1—H1N···O33^{iii} hydrogen bonds (see Table 3 for hydrogen-bond details and symmetry code), established between the protonated N atom and a phosphonate O atom of a rotation-related ligand, building a three-dimensional supramolecular network with one-dimensional channels along the [001] direction (Fig. 3). Additionally, the three-dimensional architecture is supported by weak C6—H6···O31^{iv} hydrogen bonds (see Table 3 for hydrogen-bond details and

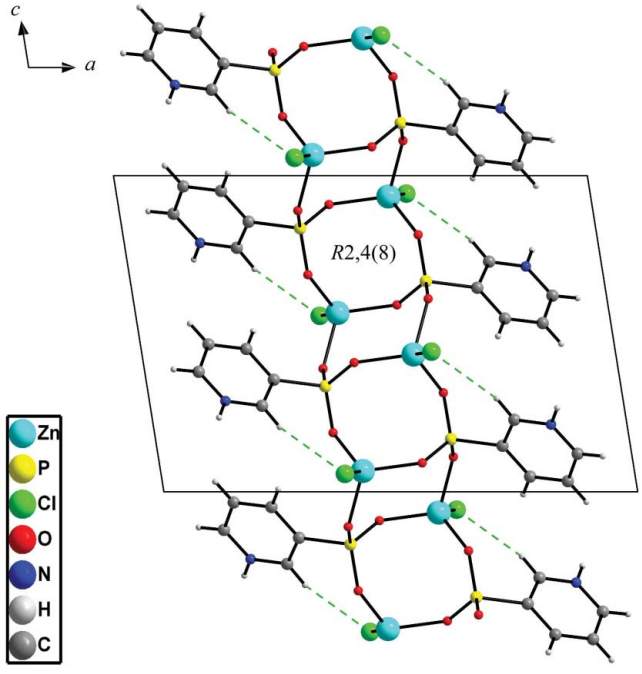

Figure 2
The ladder structure of compound (1). The C—H···Cl hydrogen bonds are drawn as dashed lines.

electronic reprint

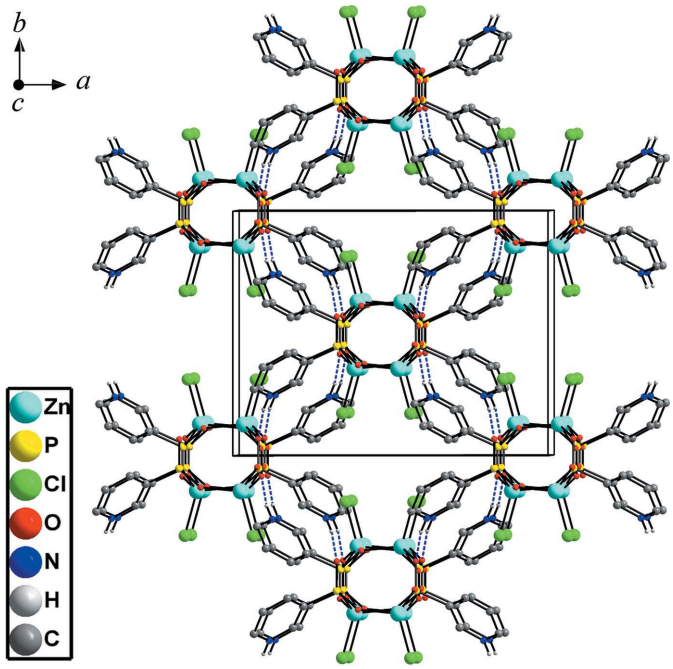

Figure 3
The three-dimensional connectivity and packing patterns of compound (1), viewed along the coordination ladders. The N—H···O hydrogen bonds are indicated as dashed lines. C-bound H atoms have been omitted for clarity.

symmetry code), donated from the aromatic C—H group towards a phosphonate O atom of an inversion-related monoanion. The pyridinium rings of neighbouring chains dovetail, resulting in offset face-to-face π–π stacking interactions. The $Cg1\cdots Cg1^{iv}$ distance is 3.668 (2) Å ($Cg1$ is the centroid of the N1/C2–C6 ring) and the slippage distance is 0.542 Å. Compound (1) possesses 17.6% of void space, as calculated by the *CrystalExplorer* program (Wolff *et al.*, 2012; Turner *et al.*, 2011) (see Fig. S2 in the *Supporting information*).

In the crystal structure of (1), each ladder chain is surrounded by four other ladders. In this way, two types of close inter-chain interactions are generated between them, as shown in Fig. 4. In the case of the M1 motif, the two adjacent chains interact with each other along the [110] and [1$\bar{1}$0] directions using the above-mentioned hydrogen bonds, *i.e.* N1—H1N···O33^{iii} and C6—H6···O31^{iv}, as well as offset face-to-face π–π stacking interactions. All this results in a significant interaction energy value of −115.2 kJ mol^{-1} between such mutually arranged chains (Table 4). According to the literature data, the obtained energy value corresponds well to the sum of typical energy values of a strong hydrogen bond, a weak one and effective π–π stacking interactions (Dunitz & Gavezzotti, 2009; Jarzembska *et al.*, 2012; Maschio *et al.*, 2011; Spackman, 2015). In turn, as far as motif M2 is concerned, the neighbouring ladders, arrayed along the [010] direction, are further apart from each other, with the closest Cl1···Cl1 contact being 5.6994 (16) Å. Consequently, the major interactions observed here are electrostatic repulsive forces, which is reflected by the positive sign of interaction energy value of 20.2 kJ mol^{-1}. These two types of most significant inter-chain

Table 4
The calculated cohesive and interaction energies for the crystal structure of compound (1).

Calculated energy[a]	Energy per ASU (kJ mol^{-1})
Interaction energy of M1	−115.2
Interaction energy of M2	20.2
Cohesive energy	−205.4

Note: (*a*) the energy calculated per ASU-equivalent fragment of a polymeric chain in the crystal structure of (1)

interactions contribute to the cohesive energy which has been calculated per polymeric fragment, consisting of four asymmetric units belonging to the unit cell and then scaled to the ASU-equivalent moiety. The total energy falling on the ASU-equivalent fragment of a polymeric chain in the crystal structure of (1) is −205.4 kJ mol^{-1} and is comparable with the cohesive energy values for molecular crystals of small organic species interacting *via* hydrogen bonds further stabilized by π–π stacking interactions (Durka *et al.*, 2012; Jarzembska *et al.*, 2013; Kutyła *et al.*, 2016; Price, 2014). It is worth noting that the above-mentioned energy value does not take into account the stabilizing interactions along the coordination chains, *i.e.* the metal–ligand ionic interactions, which should significantly contribute to the overall crystal energy, since they are often characterized by an interaction energy of 10^2 or 10^3 kJ mol^{-1} order of magnitude (Umadevi & Senthilkumar, 2016).

4. Conclusion

A new one-dimensional zinc(II) coordination polymer based on pyridin-3-ylphosphonic acid has been synthesized and characterized. The compound demonstrates a ladder structure in the solid state. Such a low-dimensional coordination structure is related to: (*a*) the presence of a chloride anion in the coordination sphere of the Zn^{II} ion, which makes this position no longer available for the bridging phosphonate ligand, and (*b*) the protonation of the N atom of the pyridyl group, which is therefore not able to bind the Zn^{II} ion. Nevertheless, adjacent ladder chains are joined together by

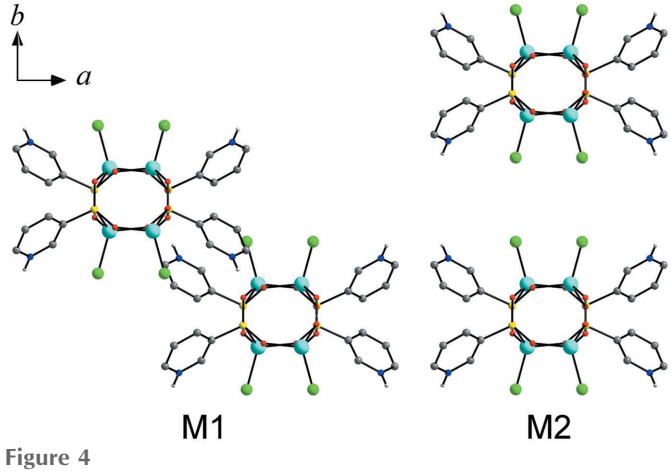

Figure 4
Schematic representation of the mutual arrangements of the polymeric chains in the crystal structure of compound (1).

electronic reprint

hydrogen-bonding and π–π stacking interactions to form a three-dimensional supramolecular channel network. It has been computed that the interaction energy between the neighbouring chains is significant and amounts to -115.2 kJ mol^{-1}. On the other hand, the cohesive energy calculated per ASU-equivalent fragment of a polymeric chain in the crystal structure is -205.4 kJ mol^{-1} and is comparable with those of molecular crystals rich in hydrogen bonds.

Acknowledgements

This work was financed by the National Science Centre. MW and VVA also gratefully acknowledge an instrument grant from the Polish Ministry of Science and Higher Education, which supported the Integrated Departmental Laboratory for Engineering and Research of Advanced Materials, where the synthesis and measurements of the FT–IR and FT–Raman spectra were performed. Calculations were carried out using resources provided by the Wrocław Centre for Networking and Supercomputing (http://wcss.pl, grant no. 285).

Funding information

Funding for this research was provided by: National Science Centre (award No. 2011/01/N/ST5/05639); Polish Ministry of Science and Higher Education (award No. 6221/IA/119/2012).

References

Ayyappan, P., Evans, O. R., Foxman, B. M., Wheeler, K. A., Warren, T. H. & Lin, W. (2001). *Inorg. Chem.* **40**, 5954–5961.

Becke, A. D. (1988). *Phys. Rev. A*, **38**, 3098–3100.

Białek, M. J., Janczak, J. & Zoń, J. (2013). *CrystEngComm*, **15**, 390–399.

Boys, S. F. & Bernardi, F. (1970). *Mol. Phys.* **19**, 553–566.

Brandenburg, K. & Putz, H. (2006). *DIAMOND*. Crystal Impact GbR, Bonn, Germany.

Cheetham, A. K., Rao, C. N. R. & Feller, R. K. (2006). *Chem. Commun.* pp. 4780–4795.

Civalleri, B., Zicovich-Wilson, C. M., Valenzano, L. & Ugliengo, P. (2008). *CrystEngComm*, **10**, 405–410.

Dovesi, R., Saunders, V. R., Roetti, R., Orlando, R., Zicovich-Wilson, C. M., Pascale, F., Civalleri, B., Doll, K., Harrison, N. M., Bush, I. J., D'Arco, P. & Llunell, M. (2009). *CRYSTAL09 User's Manual*. University of Torino, Italy.

Dunitz, J. D. & Gavezzotti, A. (2009). *Chem. Soc. Rev.* **38**, 2622–2633.

Dunning, T. H. (1989). *J. Chem. Phys.* **90**, 1007–1023.

Durka, K., Jarzembska, K. N., Kamiński, R., Luliński, S., Serwatowski, J. & Woźniak, K. (2012). *Cryst. Growth Des.* **12**, 3720–3734.

Fry, J. A., Samanamu, C. R., Montchamp, J.-L. & Richards, A. F. (2008). *Eur. J. Inorg. Chem.* pp. 463–470.

Grimme, S. (2011). *Wiley Interdiscip. Rev. Comput. Mol. Sci.* **1**, 211–228.

Horcajada, P., Gref, R., Baati, T., Allan, P. K., Maurin, G., Couvreur, P., Férey, G., Morris, R. E. & Serre, C. (2012). *Chem. Rev.* **112**, 1232–1268.

Jarzembska, K. N., Goral, A. M., Gajda, R. & Dominiak, P. M. (2013). *Cryst. Growth Des.* **13**, 239–254.

Jarzembska, K. N., Kubsik, M., Kamiński, R., Woźniak, K. & Dominiak, P. M. (2012). *Cryst. Growth Des.* **12**, 2508–2524.

Kamiński, R., Jarzembska, K. N. & Domagała, S. (2013). *J. Appl. Cryst.* **46**, 540–543.

Kitagawa, S., Kitaura, R. & Noro, S. (2004). *Angew. Chem. Int. Ed.* **43**, 2334–2375.

Kreno, L. E., Leong, K., Farha, O. K., Allendorf, M., Van Duyne, R. P. & Hupp, J. T. (2012). *Chem. Rev.* **112**, 1105–1125.

Krishnan, R., Binkley, J. S., Seeger, R. & Pople, J. A. (1980). *J. Chem. Phys.* **72**, 650–654.

Kurmoo, M. (2009). *Chem. Soc. Rev.* **38**, 1353–1379.

Kutyła, S. E., Stępień, D. K., Jarzembska, K. N., Kamiński, R., Dobrzycki, Ł., Ciesielski, A., Boese, R., Młochowski, J. & Cyrański, M. K. (2016). *Cryst. Growth Des.* **16**, 7037–7050.

Lee, J., Farha, O. K., Roberts, J., Scheidt, K. A., Nguyen, S. T. & Hupp, J. T. (2009). *Chem. Soc. Rev.* **38**, 1450–1459.

Lee, C., Yang, W. & Parr, R. G. (1988). *Phys. Rev. B*, **37**, 785–789.

Li, J.-R., Sculley, J. & Zhou, H.-C. (2012). *Chem. Rev.* **112**, 869–932.

Liu, X.-G., Bao, S.-S., Li, Y.-Z. & Zheng, L.-M. (2008). *Inorg. Chem.* **47**, 5525–5527.

Maschio, L., Civalleri, B., Ugliengo, P. & Gavezzotti, A. (2011). *J. Phys. Chem. A*, **115**, 11179–11186.

Matczak-Jon, E. & Videnova-Adrabińska, V. (2005). *Coord. Chem. Rev.* **249**, 2458–2488.

O'Keeffe, M. & Yaghi, O. M. (2012). *Chem. Rev.* **112**, 675–702.

Perry, H., Zoń, J., Law, J. & Clearfield, A. (2010). *J. Solid State Chem.* **183**, 1165–1173.

Price, S. L. (2014). *Chem. Soc. Rev.* **43**, 2098–2111.

Rigaku Oxford Diffraction (2015). *CrysAlis PRO*, *CrysAlis CCD* and *CrysAlis RED*. Rigaku Oxford Diffraction, Yarnton, Oxfordshire, England.

Samanamu, C. R., Zamora, E. N., Montchamp, J.-L. & Richards, A. F. (2008). *J. Solid State Chem.* **181**, 1462–1471.

Sheldrick, G. M. (2015*a*). *Acta Cryst.* A**71**, 3–8.

Sheldrick, G. M. (2015*b*). *Acta Cryst.* C**71**, 3–8.

Socrates, G. (2001). *Infrared and Raman Characteristic Group Frequencies: Tables and Charts*, 3rd ed., p. 229. Chichester: Wiley.

Spackman, M. A. (2015). *Cryst. Growth Des.* **15**, 5624–5628.

Suh, M. P., Park, H. J., Prasad, T. K. & Lim, D.-W. (2012). *Chem. Rev.* **112**, 782–835.

Turner, M. J., McKinnon, J. J., Jayatilaka, D. & Spackman, M. A. (2011). *CrystEngComm*, **13**, 1804–1813.

Umadevi, P. & Senthilkumar, L. (2016). *RSC Adv.* **6**, 38919–38930.

Wasson, A. E. & LaDuca, R. L. (2007). *Acta Cryst.* E**63**, m462–m464.

Wolff, S. K., Grimwood, D. J., McKinnon, J. J., Turner, M. J., Jayatilaka, D. & Spackman, M. A. (2012). *CrystalExplorer*. University of Western Australia, Crawley, Australia.

Zhou, J.-L., He, X.-Q., Liu, B., Huo, Y., Zhang, S.-C. & Chun, X.-G. (2010). *Transition Met. Chem.* **35**, 795–800.

Zoń, J., Videnova-Adrabinska, V., Janczak, J., Wilk, M., Samoc, A., Gancarz, R. & Samoc, M. (2011). *CrystEngComm*, **13**, 3474–3484.

electronic reprint

supporting information

Acta Cryst. (2017). C**73**, 363-368 [https://doi.org/10.1107/S2053229617004478]

Synthesis, structural characterization and computational studies of *catena*-poly[chlorido[μ_3-(pyridin-1-ium-3-yl)phosphonato-κ^3O:O':O'']zinc(II)]

Magdalena Wilk-Kozubek, Katarzyna N. Jarzembska, Jan Janczak and Veneta Videnova-Adrabinska

Computing details

Data collection: *CrysAlis CCD* (Rigaku Oxford Diffraction, 2015); cell refinement: *CrysAlis RED* (Rigaku Oxford Diffraction, 2015); data reduction: *CrysAlis RED* (Rigaku Oxford Diffraction, 2015); program(s) used to solve structure: SHELXT (Sheldrick, 2015); program(s) used to refine structure: *SHELXL2014* (Sheldrick, 2015); molecular graphics: *DIAMOND* (Brandenburg & Putz, 2006); software used to prepare material for publication: *SHELXL2014* (Sheldrick, 2015).

catena-Poly[chlorido[μ_3-(pyridin-1-ium-3-yl)phosphonato-κ^3O:O':O'']zinc(II)]

Crystal data

[Zn($C_5H_5NO_3P$)Cl]
M_r = 258.89
Monoclinic, $C2/c$
a = 15.260 (3) Å
b = 11.750 (2) Å
c = 10.334 (2) Å
β = 99.04 (3)°
V = 1830.0 (7) Å^3
Z = 8
F(000) = 1024
D_x = 1.879 Mg m^{-3}
D_m = 1.87 Mg m^{-3}
D_m measured by floatation
Mo $K\alpha$ radiation, λ = 0.71073 Å
Cell parameters from 1525 reflections
θ = 3.1–28.0°
μ = 3.12 mm^{-1}
T = 295 K
Parallelepiped, colourless
0.22 × 0.15 × 0.12 mm

Data collection

Kuma KM-4-CCD diffractometer
Radiation source: fine-focus sealed tube
Graphite monochromator
Detector resolution: 10.6249 pixels mm^{-1}
ω–scan
Absorption correction: multi-scan CrysAlis PRO (Rigaku Oxford Diffraction, 2015)
T_{min} = 0.832, T_{max} = 1.000
11615 measured reflections
2323 independent reflections
1633 reflections with $I > 2\sigma(I)$
R_{int} = 0.048
θ_{max} = 29.3°, θ_{min} = 3.1°
h = −20→20
k = −15→16
l = −14→12

Refinement

Refinement on F^2
Least-squares matrix: full
$R[F^2 > 2\sigma(F^2)]$ = 0.035
$wR(F^2)$ = 0.071
S = 1.00
2323 reflections
112 parameters
0 restraints
Primary atom site location: structure-invariant direct methods

electronic reprint

Secondary atom site location: difference Fourier map	$w = 1/[\sigma^2(F_o^2) + (0.0321P)^2]$ where $P = (F_o^2 + 2F_c^2)/3$
Hydrogen site location: mixed	$(\Delta/\sigma)_{max} < 0.001$
H atoms treated by a mixture of independent and constrained refinement	$\Delta\rho_{max} = 0.87$ e Å^{-3}
	$\Delta\rho_{min} = -0.45$ e Å^{-3}

Special details

Geometry. All esds (except the esd in the dihedral angle between two l.s. planes) are estimated using the full covariance matrix. The cell esds are taken into account individually in the estimation of esds in distances, angles and torsion angles; correlations between esds in cell parameters are only used when they are defined by crystal symmetry. An approximate (isotropic) treatment of cell esds is used for estimating esds involving l.s. planes.

Refinement. Refinement of F^2 against ALL reflections. The weighted R-factor wR and goodness of fit S are based on F^2, conventional R-factors R are based on F, with F set to zero for negative F^2. The threshold expression of $F^2 > 2\text{sigma}(F^2)$ is used only for calculating R-factors(gt) etc. and is not relevant to the choice of reflections for refinement. R-factors based on F^2 are statistically about twice as large as those based on F, and R- factors based on ALL data will be even larger.

Fractional atomic coordinates and isotropic or equivalent isotropic displacement parameters (Å^2)

	x	y	z	U_{iso}*/U_{eq}
Zn1	0.42687 (2)	0.36427 (3)	0.06577 (3)	0.02247 (11)
P3	0.62388 (4)	0.45705 (6)	0.16647 (7)	0.02085 (17)
Cl1	0.38814 (7)	0.18155 (8)	0.05663 (9)	0.0508 (2)
O31	0.55492 (13)	0.37996 (17)	0.0913 (2)	0.0310 (5)
O32	0.62312 (13)	0.46205 (17)	0.31321 (17)	0.0282 (5)
O33	0.62269 (12)	0.57743 (17)	0.11052 (17)	0.0270 (5)
N1	0.83978 (18)	0.2531 (3)	0.2128 (3)	0.0389 (7)
H1N	0.855 (2)	0.195 (3)	0.269 (3)	0.047*
C2	0.7639 (2)	0.3065 (3)	0.2281 (3)	0.0340 (7)
H2	0.7337	0.2840	0.2952	0.041*
C3	0.73016 (18)	0.3943 (2)	0.1455 (3)	0.0240 (6)
C4	0.7781 (2)	0.4265 (3)	0.0482 (3)	0.0352 (7)
H4	0.7576	0.4859	−0.0081	0.042*
C5	0.8562 (2)	0.3711 (3)	0.0338 (3)	0.0455 (9)
H5	0.8883	0.3925	−0.0317	0.055*
C6	0.8861 (2)	0.2815 (3)	0.1206 (4)	0.0455 (9)
H6	0.9381	0.2428	0.1126	0.055*

Atomic displacement parameters (Å^2)

	U^{11}	U^{22}	U^{33}	U^{12}	U^{13}	U^{23}
Zn1	0.02480 (18)	0.02383 (19)	0.01884 (17)	−0.00201 (15)	0.00358 (12)	−0.00099 (15)
P3	0.0219 (4)	0.0237 (4)	0.0169 (4)	−0.0008 (3)	0.0029 (3)	−0.0004 (3)
Cl1	0.0641 (6)	0.0261 (5)	0.0608 (6)	−0.0124 (4)	0.0053 (5)	0.0018 (4)
O31	0.0220 (10)	0.0352 (13)	0.0355 (12)	−0.0039 (9)	0.0036 (9)	−0.0116 (10)
O32	0.0342 (11)	0.0326 (12)	0.0187 (10)	−0.0019 (9)	0.0067 (8)	0.0014 (9)
O33	0.0348 (11)	0.0258 (11)	0.0191 (10)	−0.0001 (9)	0.0002 (9)	0.0050 (9)
N1	0.0441 (17)	0.0389 (18)	0.0324 (16)	0.0127 (14)	0.0021 (13)	−0.0010 (13)
C2	0.0324 (17)	0.0386 (19)	0.0309 (17)	0.0059 (15)	0.0042 (14)	0.0046 (15)
C3	0.0234 (14)	0.0295 (17)	0.0179 (13)	−0.0034 (12)	−0.0001 (11)	−0.0022 (12)
C4	0.0332 (17)	0.039 (2)	0.0344 (17)	−0.0022 (14)	0.0076 (14)	0.0026 (15)

electronic reprint

C5	0.0397 (19)	0.065 (3)	0.0361 (19)	−0.0040 (18)	0.0206 (16)	−0.0059 (18)
C6	0.0337 (19)	0.055 (2)	0.048 (2)	0.0138 (17)	0.0051 (17)	−0.0124 (19)

Geometric parameters (Å, º)

Zn1—O31	1.9390 (19)	N1—C2	1.348 (4)
Zn1—O32^{i}	1.9406 (19)	N1—H1N	0.91 (4)
Zn1—O33^{ii}	1.9817 (19)	C2—C3	1.386 (4)
Zn1—Cl1	2.2249 (10)	C2—H2	0.9300
P3—O31	1.508 (2)	C3—C4	1.386 (4)
P3—O32	1.5195 (19)	C4—C5	1.387 (4)
P3—O33	1.527 (2)	C4—H4	0.9300
P3—C3	1.825 (3)	C5—C6	1.411 (5)
O32—Zn1^{i}	1.9406 (19)	C5—H5	0.9300
O33—Zn1^{ii}	1.9817 (19)	C6—H6	0.9300
N1—C6	1.315 (4)		
O31—Zn1—O32^{i}	110.24 (8)	C2—N1—H1N	115 (2)
O31—Zn1—O33^{ii}	108.85 (9)	N1—C2—C3	121.2 (3)
O32^{i}—Zn1—O33^{ii}	104.83 (8)	N1—C2—H2	119.4
O31—Zn1—Cl1	110.66 (7)	C3—C2—H2	119.4
O32^{i}—Zn1—Cl1	118.03 (7)	C2—C3—C4	117.6 (3)
O33^{ii}—Zn1—Cl1	103.54 (6)	C2—C3—P3	118.6 (2)
O31—P3—O32	115.04 (12)	C4—C3—P3	123.8 (2)
O31—P3—O33	113.29 (12)	C3—C4—C5	120.7 (3)
O32—P3—O33	109.91 (12)	C3—C4—H4	119.7
O31—P3—C3	104.92 (12)	C5—C4—H4	119.7
O32—P3—C3	106.28 (12)	C4—C5—C6	118.6 (3)
O33—P3—C3	106.68 (12)	C4—C5—H5	120.7
P3—O31—Zn1	137.21 (13)	C6—C5—H5	120.7
P3—O32—Zn1^{i}	133.29 (13)	N1—C6—C5	119.6 (3)
P3—O33—Zn1^{ii}	130.42 (12)	N1—C6—H6	120.2
C6—N1—C2	122.4 (3)	C5—C6—H6	120.2
C6—N1—H1N	123 (2)		

Symmetry codes: (i) −*x*+1, *y*, −*z*+1/2; (ii) −*x*+1, −*y*+1, −*z*.

Hydrogen-bond geometry (Å, º)

D—H···*A*	*D*—H	H···*A*	*D*···*A*	*D*—H···*A*
C2—H2···Cl1^{i}	0.93	2.85	3.756 (3)	164
N1—H1*N*···O33^{iii}	0.91 (4)	1.85 (4)	2.756 (4)	175 (3)
C6—H6···O31^{iv}	0.93	2.57	3.134 (4)	120

Symmetry codes: (i) −*x*+1, *y*, −*z*+1/2; (iii) −*x*+3/2, *y*−1/2, −*z*+1/2; (iv) −*x*+3/2, −*y*+1/2, −*z*.

electronic reprint